

## Strengthening of Reentrant Pinning by Collective Interactions in the Peak Effect

J. Lefebvre, M. Hilke, and Z. Altounian

*Department of Physics, McGill University, Montréal, Canada H3A 2T8*

(Received 22 April 2009; published 26 June 2009)

Since it was first observed about 40 years ago [A. B. Pippard, Proc. R. Soc. A **216**, 547 (1953)], the peak effect has been the subject of extensive research mainly impelled by the desire to determine its exact mechanisms. Despite these efforts, a consensus on this question has yet to be reached. Experimentally, the peak effect indicates a transition from a depinned vortex phase to a reentrant pinning phase at a high magnetic field. To study the effects of intrinsic pinning on the peak effect, we consider  $\text{Fe}_x\text{Ni}_{1-x}\text{Zr}_2$  superconducting metallic glasses in which the vortex pinning force varies depending on the Fe content and in which a huge peak effect is seen. The results show that the peak effect broadens with decreasing pinning force. Typically, pinning is increased by pinning centers, but here we show that reentrant pinning is due to the strengthening of interactions and collective effects (while decreasing pinning strength).

DOI: 10.1103/PhysRevLett.102.257002

PACS numbers: 74.25.Qt, 74.25.Dw, 74.25.Op, 74.25.Sv

Vortices in type II superconductors form a correlated system of interacting particles which can be studied as a function of particle density or driving force by simply tuning the external magnetic field or driving current. While elastic vortex-vortex interactions tend to order the system, vortex-pin interactions result in disorder. An ever intriguing phenomena resulting from this competition between elastic and plastic interactions is the peak effect (PE): an anomalous peak in the critical current  $J_c$  (or dip in resistance). This peak appears with increasing temperature or magnetic field just below the transition to the normal state in some conventional superconductors [1–6] and at a lower field below  $B_{c2}$  in high  $T_c$  superconductors [7]. In type II superconductors, vortices will depin under the action of a driving force larger than the critical force. As a result of vortex motion, a dissipative voltage proportional to  $\mathbf{E} = \bar{\mathbf{v}} \times \mathbf{B}$ , where  $\bar{\mathbf{v}}$  is the average vortex velocity, will be induced and a nonzero resistance will be measured. In the PE, vortices are pinned again, resulting in a decrease of the resistance or an increase of the critical current. The origin of the PE is still under debate. Early, it was suggested to arise due to the softening of the elastic moduli of the vortex lattice [1] and to a decrease of the correlation volume  $V_c$  in the collective pinning theory of Larkin and Ovchinnikov [8]. It has also been proposed to be the signature of a disorder-induced or a thermally induced order-disorder transition [5,9–12]. However, it has equally been said to occur naturally at the crossover between a weak to a strong vortex pinning regime [13]. It could also simply appear depending on the strength and density of pinning centers and their competing action depending on the magnetic field and temperature [14–16]. In general, the dependence of the PE on disorder is strongly dependent on the pinning mechanism: single vortex pinning versus collective pinning.

In this work, we investigate how the PE depends on pinning strength by using a series of  $\text{Fe}_x\text{Ni}_{1-x}\text{Zr}_2$  metallic

glasses with  $x$  from 0 to 0.6, since changing  $x$  modifies the pinning properties. The extreme purity and absence of long range order due to the amorphous nature of these glasses confers on them extremely weak pinning properties ( $J_c \leq 0.4 \text{ A/cm}^2$ ) which make them ideal systems to study vortex phases and vortex motion. Pinning in these glasses is collective. In Ref. [6], a huge PE, larger than in other weakly pinned amorphous systems [2,4,17,18], was observed in a sample of  $\text{Fe}_{0.3}\text{Ni}_{0.7}\text{Zr}_2$ . Since the critical current density in these alloys is at least 10 times smaller than seen in other amorphous alloys [2,4,17,18], this provides an ideal case study for the weak-pinning limit.

The  $\text{Fe}_x\text{Ni}_{1-x}\text{Zr}_2$  superconducting glasses are obtained by melt spinning, as described in Ref. [19]. Resistance measurements are performed in the standard four-probe technique through soldered indium contacts using a resistance bridge providing ac current at 15.9 Hz in a  $^3\text{He}$  refrigerator and a dilution refrigerator.

The pinning force density is determined from  $f_p = J_c B$  and is shown in the inset in Fig. 1 as a function of Fe content  $x$  at a magnetic field  $B = 0.15B_{c2}$ , where  $B_{c2}$  is the upper critical field. The critical current density  $J_c$  is defined when the resistance reaches  $0.5 \text{ m}\Omega$ , which is close to our experimental resolution. As can be seen in Fig. 1, increasing the Fe content in these glasses results in an important decrease of the pinning force density;  $f_p$  is about a factor of 5 smaller for  $x = 0.5$  and  $0.6$  than it is for  $x = 0.1$ . This dependence stems from a substantial increase of the vortex core and size with increasing  $x$ . As calculated from expressions for superconductors in the dirty limit [4], in  $x = 0$ ,  $\xi_{\text{GL}}(0) = 8.1 \text{ nm}$  and  $\lambda(0) = 0.87 \mu\text{m}$ , which, respectively, almost doubles and triples in  $x = 0.6$  [20]. This yields the relationship between  $\xi_{\text{GL}}(0)$  and  $\lambda(0)$  and  $f_p$ , shown in Fig. 1. A strong decrease of the pinning force density with increasing coherence length was also predicted by Larkin and Ovchinnikov (LO) [8], who obtained for 3D collective pinning the dependence

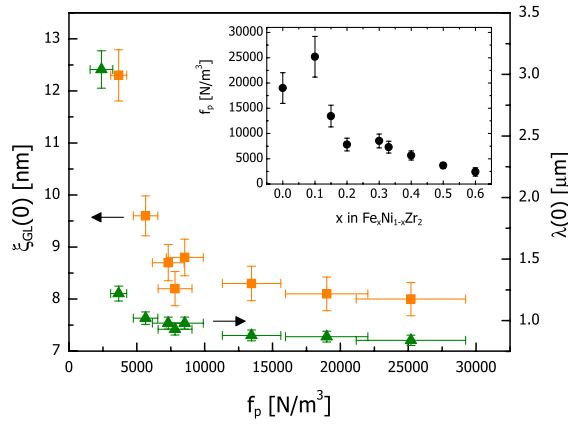


FIG. 1 (color online). Ginzburg-Landau (GL) coherence length  $\xi_{GL}(0)$  (orange squares) and penetration depth  $\lambda(0)$  (green triangles) as a function of the pinning force density  $f_p$ . Inset:  $f_p$  as a function of Fe content  $x$  in  $Fe_xNi_{1-x}Zr_2$ .

$$f_p = \frac{n^2 \langle f^2 \rangle^2}{10B^2 C_{66}^2 \xi^3}, \quad (1)$$

where  $n$  and  $f$  are the density and strength of pins, respectively, and  $C_{66}$  is the shear modulus which describes the elasticity of the vortices. The decrease of  $f_p$  with increasing  $\xi$  is readily understood considering that, for identical vortex number density, vortex overlap is enhanced for large  $\xi$  and  $\lambda$ , thereby increasing collective interactions between vortices which tend to order the system and reduce pinning. Indeed, according to the LO collective pinning theory [8], the scale of vortex interactions can be described by a correlation volume  $V_c = R_c^2 L_c$ , where  $R_c$  and  $L_c$  are the correlation radius and length, respectively.  $R_c$  increases with  $\xi$  according to  $R_c = 4\pi^{1/2} B C_{66}^{3/2} \xi^2 / n \langle f^2 \rangle$ , which then results in a decrease of the pinning force

$$f_p = \left( \frac{n \langle f^2 \rangle}{V_c} \right)^{1/2}. \quad (2)$$

According to the LO collective pinning theory, in the weak-pinning limit and for high magnetic fields where the number of vortices greatly surpasses the number of defects, reentrant pinning in the peak effect results from the pinning of mobile vortices through collective interactions with pinned vortices. Hence, enhanced collective interactions strengthen the peak effect.

The evolution of pinning strength and collective vortex interactions with Fe content in  $Fe_xNi_{1-x}Zr_2$  evidenced above allows us to study how the peak effect depends on collective effects. As seen in measurements of the resistance as a function of magnetic field on samples with  $x = 0, 0.3,$  and  $0.5$  in Fig. 2, the dip in resistance characterizing this  $B$ -induced reentrant pinning phase changes from thin and shallow in the more strongly pinned  $NiZr_2$  to very broad and deep in the more weakly pinned  $Fe_{0.5}Ni_{0.5}Zr_2$ . In the latter case, the resistance even decreases back to zero in the peak effect and a large reentrant superconducting phase

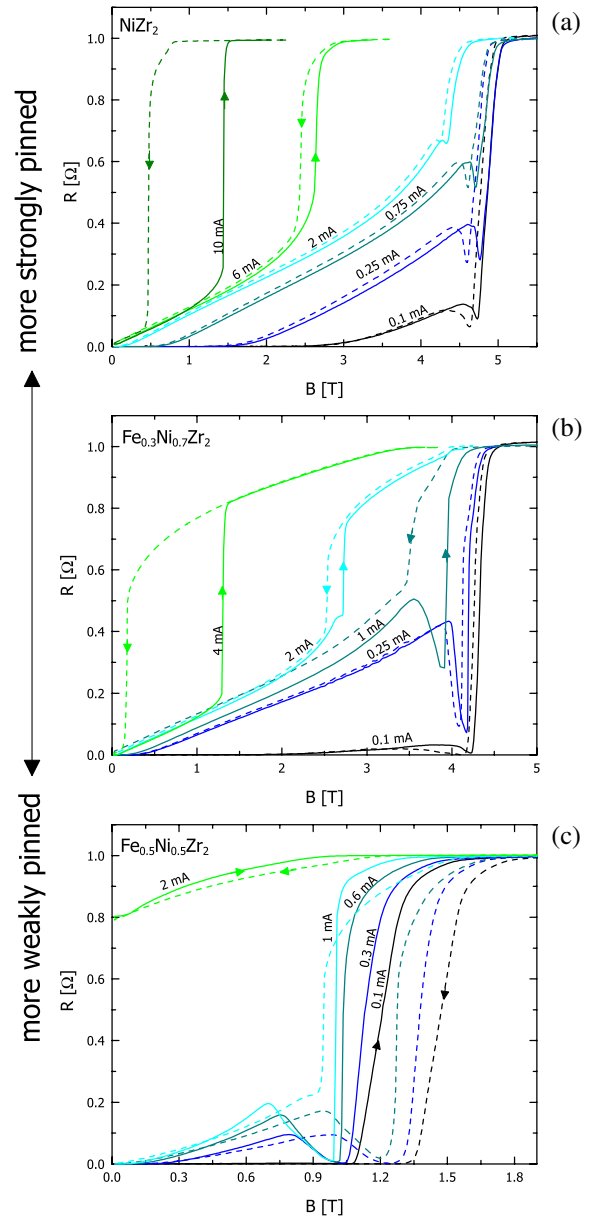


FIG. 2 (color online). Resistance vs magnetic field for different driving currents as shown at  $T \approx 0.33$  K measured on different metallic glasses of varying pinning properties. (a)  $NiZr_2$  (more strongly pinned); (b)  $Fe_{0.3}Ni_{0.7}Zr_2$ ; (c)  $Fe_{0.5}Ni_{0.5}Zr_2$  (more weakly pinned).

is seen. In crystals of  $2H-NbSe_2$  containing a large amount of quenched disorder introduced as Fe impurities and showing stronger point pinning properties, a broadening of the PE has been observed before [21]. This is mainly due to an increased inhomogeneous pinning, where the preferred pinning of single vortices impedes the others. This can be contrasted to our amorphous alloys in which pinning is weak but collective and PE broadening is seen with decreasing pinning force and growing collective effects.

A similar broadening of the PE with  $x$ , with accompanied deepening of the resistance dip at the PE, is also

observed in resistance measurements performed as a function of temperature in a fixed  $B$  field (Fig. 3). This important observation confirms that PE broadening is indeed attributable to the augmentation of collective interactions and not due to the presence of inhomogeneities in the material. This confirmation is essential here because, in Refs. [20,22], we have evidenced the presence of structural inhomogeneities, especially in alloys with a relatively large Fe content  $x = 0.5$  and  $x = 0.6$ , which causes an inhomogeneous distribution of vortices upon entry and exit in a  $B$  field sweep. This effect is dynamic; in a constant magnetic field, the vortex distribution eventually becomes homogeneous as the vortices diffuse throughout the more weakly and strongly pinned regions of the material. As a result, during a temperature sweep in a constant  $B$  field, the flux distribution remains homogeneous as the number of vortices in the sample is fixed. It was suggested by Brandt [23] that a PE could arise in superconductors in which large inhomogeneities, with  $T_c$  higher than that of the main phase, are present. An enhancement of the PE in simulated systems of weakly pinned interacting polydisperse Yukawa particles was also observed by Reichhardt and Reichhardt [24].

Having established that the characteristics of the PE as a function of  $x$  are equivalently observed in  $B$  field and temperature sweeps, we complete our analysis from measurements performed as a function of the  $B$  field because these results are more readily obtained. A typical  $R$  vs  $B$  trace is shown in Fig. 4(a). Following the naming scheme of Ref. [6] to identify vortex phases, we distinguish the superconducting phase where  $R = 0$  at low  $B$  field, followed at higher field by a depinned vortex phase called depinning 1, the onset of which is defined when the resistance reaches  $0.5 \text{ m}\Omega$ . In Refs. [25,26], we have demonstrated that the depinning 1 phase is characterized by the long range ordered moving Bragg glass phase [27]. At still higher  $B$  field, a reentrant pinning phase is seen; the onset of this phase is defined when  $dR/dB = 0$ , and its termination is defined at the position in  $B$  where the resistance

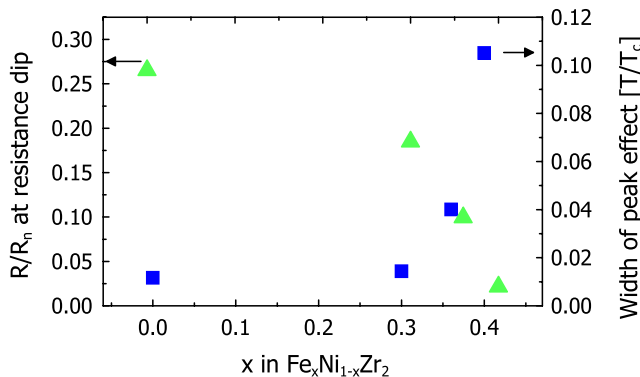


FIG. 3 (color online). Lowest resistance reached in the resistance dip (PE) (green triangles, left axis) and width of the peak effect (blue squares, right axis) as measured in temperature sweeps in a fixed  $B$  field of 2 T with  $I = 0.1 \text{ mA}$ .

reaches the same value as at the onset of the pinning phase. The end of the pinning phase marks the onset of the depinning 2 phase, which we have shown in Ref. [25] exists even in the lowest driving current regime. This phase has the smectic order characteristic of the moving transverse glass [27] in which the orientation of channels in which vortices flow can vary suddenly depending on the driving force and vortex density. Finally,  $B_{c2}$  is defined at the point of strongest negative curvature before reaching the normal state.

Extracting the boundaries of vortex phases according to the definitions above from  $R$  vs  $B$  traces measured at a constant current density  $J \approx 1.8 \text{ A/cm}^2$ , we obtain the phase diagram of Fig. 4(b). For all alloys, this current density corresponds to a regime in which we observe a peak effect, and never a direct transition from the depinning 1 to the depinning 2 phase as visible, for example, in the  $I = 10 \text{ mA}$  trace in Fig. 2(a). In the diagram, the superconducting and peak effect phases are represented

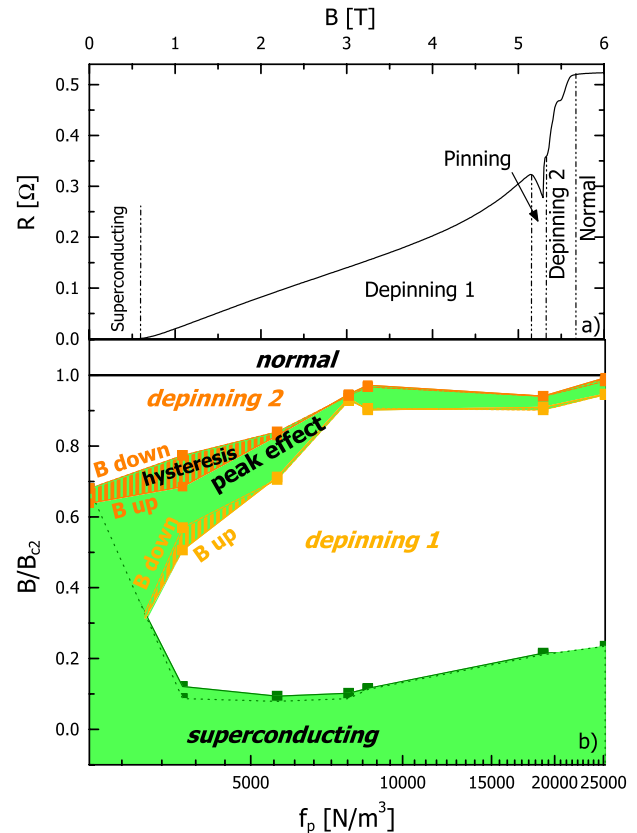


FIG. 4 (color online). (a)  $R$  vs  $B$  trace measured at  $T = 0.35 \text{ K}$  on  $\text{Fe}_{0.1}\text{Ni}_{0.9}\text{Zr}_2$  with  $I = 1 \text{ mA}$  showing how different vortex phases are defined. (b) Phase diagram of vortex dynamics as a function of pinning force density. The phase boundaries are defined as described in the text and extracted from  $R$  vs  $B$  data measured with  $J \approx 1.8 \text{ A/cm}^2$  for each alloy composition. The solid lines represent phase boundaries obtained in increasing  $B$  field sweeps, while the dotted lines are for decreasing field sweeps. In this manner, we can identify regions of hysteresis (hatched areas).

by filled green areas. These two phases merge in the most weakly pinned sample ( $x = 0.6$ ) in which no PE is visible and the vortices remain pinned up to the depinning 2 phase. A downward bending of the pinning phase toward lower reduced field  $b = B/B_{c2}$  with decreasing pinning force is observed. In the PE, an amorphization of the vortex lattice with collapse of  $V_c$  occurs [8] due to a softening of the elastic moduli [1], which increases pinning. In the high  $B$  field range where the PE appears, the size of the correlation radius  $R_c$  becomes comparable to  $\xi$  and to the intervortex distance  $a$ . In the large coherence length limit, where  $R_c$  is also largest, the onset of the peak effect can occur at lower magnetic field where  $a$  is larger, which explains this downward bending of the pinning phase toward lower  $b$  in this limit. In the most weakly pinned sample,  $V_c$  presumably becomes so large due to the large  $\xi$  and  $\lambda$  that, even at very low  $B$ , coherent pinning of these large vortex bundles does not permit depinning. As a result, the sample remains in the pinning phase up to the transition to the depinning 2 phase. The broadening of the PE phase with decreasing  $f_p$  (or increasing  $V_c$ ) is readily seen from the phase diagram and confirms that reentrant pinning is strengthened by collective vortex interactions. This also infers that collective vortex interactions cause the PE in these materials.

In the phase diagram of Fig. 4(b), the solid and dotted lines represent transitions obtained in increasing and decreasing magnetic field sweeps, respectively. As a result, regions of hysteresis become visible, as highlighted by the orange and yellow hatched areas in the weak-pinning range. These hysteresis regions are not stable and depend on the  $B$  field sweep rate. They arise due to the inhomogeneous distribution of vortices resulting from structural inhomogeneities discussed earlier. However, even by ignoring the hysteresis regions, the broadening of the PE with decreasing pinning force is obvious. A large broadening of the depinning 2 phase is also visible in the low pinning force region of the phase diagram of Fig. 4(b). This broadening is partly due to the increasingly two-phase character of these alloys. An increase of the  $B_{c2}$  transition width is common in inhomogeneous superconductors. At this stage, it is not known how the intrinsic pinning force and collective vortex interactions affect the smectic order characteristic of the depinning 2 phase and if it could cause its widening.

In summary, we have presented the pinning force dependence of the peak effect based on measurements in the metallic glasses  $\text{Fe}_x\text{Ni}_{1-x}\text{Zr}_2$ . It was shown that, in this metallic glass series, the intrinsic pinning force decreases with Fe content as the coherence length and penetration depth increase, as well as collective vortex interactions. Then a strengthening of the peak effect, which broadens to eventually fill the whole space below the transition to the

depinning 2 phase in the most weakly pinned sample, was seen with decreasing pinning force. These observations confirm that collective vortex interactions are at the origin of the peak effect phenomenon in these weakly pinned metallic glasses.

- 
- [1] A. B. Pippard, Proc. R. Soc. A **216**, 547 (1953).
  - [2] T. G. Berlincourt, R. R. Hake, and D. H. Leslie, Phys. Rev. Lett. **6**, 671 (1961).
  - [3] E. S. Rosenblum, S. H. Autler, and K. H. Goen, Rev. Mod. Phys. **36**, 77 (1964).
  - [4] P. H. Kes and C. C. Tsuei, Phys. Rev. B **28**, 5126 (1983).
  - [5] Y. Paltiel *et al.*, Phys. Rev. Lett. **85**, 3712 (2000).
  - [6] M. Hilke, S. Reid, R. Gagnon, and Z. Altounian, Phys. Rev. Lett. **91**, 127004 (2003).
  - [7] W. K. Kwok, J. A. Fendrich, C. J. van der Beek, and G. W. Crabtree, Phys. Rev. Lett. **73**, 2614 (1994).
  - [8] A. I. Larkin and Y. N. Ovchinnikov, J. Low Temp. Phys. **34**, 409 (1979).
  - [9] G. P. Mikitik and E. H. Brandt, Phys. Rev. B **64**, 184514 (2001).
  - [10] C. J. van der Beek, S. Colson, M. V. Indenbom, and M. Konczykowski, Phys. Rev. Lett. **84**, 4196 (2000).
  - [11] S. R. Park, S. M. Choi, D. C. Dender, J. W. Lynn, and X. S. Ling, Phys. Rev. Lett. **91**, 167003 (2003).
  - [12] T. Klein *et al.*, Nature (London) **413**, 404 (2001).
  - [13] G. Blatter, V. B. Geshkenbein, and J. A. G. Koopmann, Phys. Rev. Lett. **92**, 067009 (2004).
  - [14] X. B. Xu, H. Fangohr, X. N. Xu, M. Gu, Z. H. Wang, S. M. Ji, S. Y. Ding, D. Q. Shi, and S. X. Dou, Phys. Rev. Lett. **101**, 147002 (2008).
  - [15] M. Werner, F. M. Sauerzopf, H. W. Weber, and A. Wisniewski, Phys. Rev. B **61**, 14795 (2000).
  - [16] W. K. Kwok, J. A. Fendrich, C. J. van der Beek, and G. W. Crabtree, Phys. Rev. Lett. **73**, 2614 (1994).
  - [17] J. M. E. Geers, C. Attanasio, M. B. S. Hesselberth, J. Aarts, and P. H. Kes, Phys. Rev. B **63**, 094511 (2001).
  - [18] R. Wördenweber, P. H. Kes, and C. C. Tsuei, Phys. Rev. B **33**, 3172 (1986).
  - [19] M. Dikeakos, Z. Altounian, D. H. Ryan, and S. J. Kwon, J. Non-Cryst. Solids **250**, 637 (1999).
  - [20] J. Lefebvre, M. Hilke, and Z. Altounian, Phys. Rev. B **79**, 184525 (2009).
  - [21] S. S. Banerjee *et al.*, Phys. Rev. B **59**, 6043 (1999).
  - [22] J. Lefebvre, M. Hilke, Z. Altounian, K. W. West, and L. N. Pfeiffer, Phys. Rev. B **79**, 184524 (2009).
  - [23] E. H. Brandt, Phys. Status Solidi B **71**, 277 (1975).
  - [24] C. Reichhardt and C. J. O. Reichhardt, Phys. Rev. E **77**, 041401 (2008).
  - [25] J. Lefebvre, M. Hilke, R. Gagnon, and Z. Altounian, Phys. Rev. B **74**, 174509 (2006).
  - [26] J. Lefebvre, M. Hilke, and Z. Altounian, Phys. Rev. B **78**, 134506 (2008).
  - [27] P. Le Doussal and T. Giamarchi, Phys. Rev. B **57**, 11356 (1998).